Magneto-Thermo-Elastic Stresses and Perturbation of Magnetic Field Vector in a Thin Functionally Graded Rotating Disk

A. Ghorbanpour Arani[1,2,*], S. Amir[1]

[1]*Faculty of Mechanical Engineering, University of Kashan, Kashan, Islamic Republic of Iran*
[2]*Institute of Nanoscience & Nanotechnology, University of Kashan, Kashan, Islamic Republic of Iran*

ABSTRACT

In this paper, a semi-analytical solution for magneto-thermo-elastic problem in an axisymmetric functionally graded (FG) hollow rotating disk with constant thickness placed in uniform magnetic and thermal fields with heat convection from disk's surfaces is presented. Solution for stresses and perturbation of magnetic field vector in a thin FG rotating disk is determined using infinitesimal theory of magneto-thermo-elasticity under plane stress conditions. The material properties except Poisson's ratio are modeled as power-law distribution of volume fraction. The non-dimensional distribution of temperature, displacement, stresses and perturbation of magnetic field vector throughout radius are determined. The effects of the material grading index and the magnetic field on the stress and displacement fields are investigated. The results of stresses and radial displacements for two different boundary conditions are compared with the case of a thin FG rotating disk with the same loading and boundary conditions but in the absence of magnetic field. It has been found that imposing a magnetic field significantly decreases tensile circumferential stresses. Therefore, the fatigue life of the disk will be significantly improved by applying the magnetic field. The results of this investigation can be used for optimum design of rotating disks.

© 2011 IAU, Arak Branch. All rights reserved.

Keywords: FG rotating disk; Magneto-thermo-elastic stress; Heat convection; Perturbation of magnetic field vector

1 INTRODUCTION

THE functionally graded materials (FGMs) have attracted much attention in recent years. In such materials, the properties are varied continuously according to a function of position along certain direction(s) of the structure. Indeed, FGMs are combinations of two material phases that has an intentional graded transition from one material at one surface to another material at the opposite surface.

The first idea for producing FGMs was their application in high temperature environment and their forming ability. These materials which are mainly constructed to operate in high temperature environments find their application in nuclear reactors, chemical laboratories, aerospace, turbine rotors, flywheels and pressure vessels. As the use of FGMs increases, new methodologies need to be developed to characterize, analyze and design structural components made of these materials. There are some studies dealing with elastic and thermo-elastic problems of FGMs components but few studies can be found on the magneto-thermo-elastic behavior under heat convection of such components in the literature. Suresh and Mortensen [1] have provided an introduction to the fundamentals of FGMs. Lutz and Zimmerman [2, 3] obtained analytical solutions for the stresses in spheres and cylinders made of

---

* Corresponding author. Tel.: +98 9131626594 ; Fax: +98 361 55912424.
  E-mail address: aghorban@kashanu.ac.ir (A.Ghorbanpour Arani).

FGMs. They considered thick spheres and cylinders under radial thermal loads with a linear composition of the constituent materials. Hosseini Kordkheili and Naghdabadi [4] investigated the relative influences of basic factors such as property gradation, inertia and thermal loadings on stresses and deformation in a FG rotating disk. Obata and Noda [5] studied the thermal stresses in a FG circular hollow cylinder and a hollow sphere using the perturbation method assuming one-dimensional steady-state conditions.

Dai and Fu [6] considered the magneto-thermo-elastic problem of FGM hollow structures subjected to mechanical loads. They assumed that the material properties to be a simple form of power-law variation through the structure's wall thickness. Using the infinitesimal theory of elasticity, Dai et al. [7] analyzed the magneto-thermo-elastic behavior of FGM cylindrical and spherical vessels subjected to an internal pressure and a uniform magnetic field.Ghorbanpour et al. [8] presented an analytical method to obtain the response of magneto-thermo-elastic stress and perturbation of the magnetic field vector for a thick-walled spherical vessel made of FGMs. They studied the effect of magnetic field vector and material in-homogeneity on the stresses in FGM hollow sphere. They concluded that the analyses and numerical results presented in their article are accurate and reliable and may be used as a reference to solve other dynamic coupled problems in an FGM hollow sphere placed in a uniform magnetic field, subjected to mechanical load and thermal shock. Ghorbanpour et al. [9] presented a closed-form solution for one-dimensional magneto-thermo-elastic problem in a FGM hollow sphere placed in uniform magnetic and temperature fields subjected to an internal pressure using the infinitesimal theory of magneto-thermo-elasticity. The results of their study are applicable for designing optimum FGM hollow spheres. Tang [10] presented an elastic solution for anisotropic rotating disks. Ruhi et al. [11] presented a semi-analytical solution for thick-walled finitely-long cylinders made of FGMs under thermo mechanical load. Farshi et al. [12] used the variable material properties method (VMP) to obtain an optimum profile of an inhomogeneous nonuniform rotating disk with plastic deformation. Time-dependent creep stress redistribution analysis of a thick-walled FGM cylinder placed in uniform magnetic and temperature fields and subjected to an internal pressure was investigated by Loghman et al. [13]. Bayat et al. [14] presented a theoretical solution for thermoelastic analysis of functionally graded (FG) rotating disk with variable thickness based on first-order shear deformation theory. Ghorbanpour et al. [15] presented a semi-analytical solution of magneto-thermo-elastic stresses for functionally graded variable thickness rotating disks placed in uniform magnetic and temperature fields.

However, so far, investigation on magneto-thermo-elastic stresses and perturbation of magnetic field vector in a thin functionally graded rotating disk under conduction and convection heat transfer has not been found in the literature. Moreover, because of the important control of the distribution of rotating disk in structures e.g. turbine blades, this study can be useful to control of the behavior of rotating disk by magnetic filed. Motivated by these considerations, the need for investigation of the functionally graded rotating disk Fig.1 under magnetic field and convection heat transfer from its surfaces with the power-law distribution material properties is very much felt. Plane stress condition and the symmetry with respect to the axis and the mid-plane are assumed. The main objective of this study is to investigate the effect of magnetic field and temperature changes on the stresses and deformation behavior of FG rotating disks. The effect of boundary conditions and the material property gradation are also investigated. Based on power-law distribution for the material properties of the constituent components, a semi-analytical method is employed in this paper to obtain the magneto-thermo-elastic solutions for the non-dimensional variables such as temperature, displacement, stresses and perturbation of magnetic field vector in the FG disks.
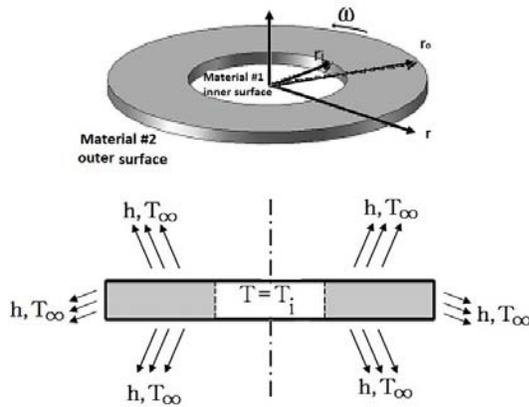
Fig. 1
Configuration of a thin FG hollow rotating disk.

2 PROPERTY GRADATION

In some studies, the variation of properties are modeled as power-law or exponential function of radius. In this study, are assumed to be in the following form [14, 15]:

$$P(r) = (P_o - P_i)\left(\frac{r - r_i}{r_o - r_i}\right)^n + P_i, \qquad r_i < r < r_o \tag{1}$$

where P_i and P_o denote the property values at the inner and outer surfaces of the disk, r_i and r_o are the inner and outer radii of the FG rotating disk, respectively. Here, for brevity, symbol P_r has been used for the functions $P(r)$. Noting that $n \geq 0$ is the volume fraction exponent which called grading index that indicates the material variation profile along the radius. This form of volume fraction can justify the concept of mixture between two materials that make FGM.

In this study, all parameters including material properties and boundary conditions are used in non-dimensional form by introducing the following set of variables:

$$R = \frac{r}{r_o}, \qquad R_i = \frac{r_i}{r_o}, \qquad R_i < R < 1$$

$$\overline{P_R} = \overline{P(R)} = (1 - \overline{P_{R_i}})\left(\frac{R - R_i}{1 - R_i}\right)^n + \overline{P_{R_i}}, \qquad \overline{P_{R_i}} = \frac{P(r_i)}{P(r_o)} \tag{2}$$

3 BOUNDARY CONDITIONS

The following traction conditions on the inner and outer surfaces of the rotating disk must be satisfied.

3.1 Hollow disk with free-free boundary condition

$$\sigma_r = 0, \qquad r = r_i$$
$$\sigma_r = 0, \qquad r = r_o \tag{3}$$

3.2 Hollow disk with fixed-free boundary condition

$$u = 0, \qquad r = r_i$$
$$\sigma_r = 0, \qquad r = r_o \tag{4}$$

The non-dimensional forms of the above boundary conditions are:

a) free-free boundary condition

$$\overline{\sigma}_R = 0, \qquad R = R_i$$
$$\overline{\sigma}_R = 0, \qquad R = 1 \tag{5}$$

b) fixed-free boundary condition

$$U = 0, \qquad R = R_i$$
$$\overline{\sigma}_R = 0, \qquad R = 1 \tag{6}$$

4   HEAT CONDITION AND CONVECTION PROBLEM

Consider a thin axisymmetric FG hollow rotating disk with constant thickness and thermal conductivity $k(r)$ and convection heat transfer from its surfaces. It is assumed that the tempreture at inner surface of disk to be constant (T_i), the outer $(r = r_o)$, top and bottom surfaces are exposed to free convection to the ambient (h, T_∞). The non-homogeneous thermal conductivity is a power-law function of volume fraction as following [14]:

$$k(r) = (k_o - k_i)\left(\frac{r - r_i}{r_o - r_i}\right)^n + k_i \tag{7}$$

The first law of thermodynamics for energy balance equation in the steady-state condition with heat convection for an axisymmetric FG one-dimensional disk, without considering energy generation, is given by [14]:

$$\frac{1}{r}\frac{\partial}{\partial r}\left[rk(r)\frac{\partial T}{\partial r}\right] - \frac{2h}{z_0}(T(r) - T_\infty) = 0 \tag{8}$$

which h is the convection heat transfer coefficient and the ambient temperature is T_∞. The thermal boundary conditions for this rotating disk are:

$$T(r)\Big|_{r=r_i} = T_i$$
$$-k(r_o)\frac{\partial T}{\partial r}\Big|_{r=r_o} = h(T(r_o) - T_\infty) \tag{9}$$

Based on heat transfer statements, the non-dimensional temperature difference is defined as:

$$\overline{\Delta T}_R = \frac{T - T_\infty}{T_i - T_\infty} \tag{10}$$

Substituting non-dimensional form of variable Eq. (7) into heat conduction Eq. (8) yields:

$$\frac{\mathrm{d}^2 \overline{\Delta T_R}}{\mathrm{d}R^2} + \left(\frac{1}{R} + \frac{1}{\overline{K_R}} \frac{\mathrm{d}\overline{K_R}}{\mathrm{d}R}\right) \frac{\mathrm{d}\overline{\Delta T_R}}{\mathrm{d}R} - r_o^2 \frac{2h}{z_0 k_0 \overline{K_R}} \overline{\Delta T_R} = 0 \tag{11}$$

where $\overline{K_R}$ is non-dimensional thermal conductivity, which is defined according to Eq. (2). Eq. (11) is a second order ODE with variable coefficients. Due to complication of coefficients, semi-analytical method for solution has been used. For this purpose, the solution domain is divided into several divisions as shown in Fig. 2 and the coefficients of Eq. (11) are evaluated at $R^{(k)}$, mean radius of kth division and the ODE with constant coefficients valid only in kth sub-domain turns out to be;

$$\left(\frac{\mathrm{d}^2}{\mathrm{d}R^2} + \overline{c}^{(k)} \frac{\mathrm{d}}{\mathrm{d}R} - \frac{2hr_o^2}{z_0 k_0 \overline{K_{R^{(k)}}}}\right) \overline{\Delta T_{R^{(k)}}} = 0 \tag{12}$$

where

$$\overline{c}^{(k)} = \frac{1}{R^{(k)}} + \frac{1}{\overline{K_{R^{(k)}}}} \frac{\mathrm{d}\overline{K_R}}{\mathrm{d}R}\bigg|_{R=R^{(k)}}, \qquad k = 1, 2, ..., m \tag{13}$$

Now the 2nd order ODE with variable coefficients is converted into 2nd order ODE with constant coefficients for each division. The exact solution for these types of ODEs can be written as:

$$\overline{\Delta T_{R^{(k)}}} = \overline{X_1}^{(k)} \exp(\zeta_1^{(k)} \overline{R^{(k)}}) + \overline{X_2}^{(k)} \exp(\zeta_2^{(k)} \overline{R^{(k)}}) \tag{14a}$$

and

$$\zeta_1^{(k)}, \zeta_2^{(k)} = \frac{\overline{c}^{(k)} \pm \sqrt{(\overline{c}^{(k)})^2 - 4\frac{2hr_o^2}{z_0 k_0 \overline{K_{R^{(k)}}}}}}{2} \tag{14b}$$

where $\overline{X_1}^{(k)}$ and $\overline{X_2}^{(k)}$ are unknown constants for kth division. These unknowns are determined by satisfying the essential boundary conditions and between each two adjacent sub-domains. In addition, the continuity conditions for temperature and heat flux must be imposed as follows:

$$\overline{\Delta T_R}\bigg|_{R=R^k + \frac{t^k}{2}} = \overline{\Delta T_R}\bigg|_{R=R^{k+1} - \frac{t^{k+1}}{2}}, \qquad \frac{\mathrm{d}\overline{\Delta T_R}}{\mathrm{d}R}\bigg|_{R=R^k + \frac{t^k}{2}} = \frac{\mathrm{d}\overline{\Delta T_R}}{\mathrm{d}R}\bigg|_{R=R^{k+1} - \frac{t^{k+1}}{2}} \tag{15}$$

and thermal boundary conditions are:

$$\overline{\Delta T_R} = \overline{\Delta T_i} = 1 \text{ at } R = R_i,$$
$$\overline{\Delta T_R} = \overline{\Delta T_o} = \frac{T_o - T_\infty}{T_i - T_\infty} \text{ at } R = R_o = 1 \tag{16}$$

The continuity conditions Eq. (15) with thermal boundary conditions Eq. (16) lead to a set of linear algebraic equations in terms of $\overline{X_1}^{(k)}$ and $\overline{X_2}^{(k)}$. Solving these equations for $\overline{X_1}^{(k)}$ and $\overline{X_2}^{(k)}$, temperature $\overline{\Delta T_R}$ can be obtained in each sub-domain.
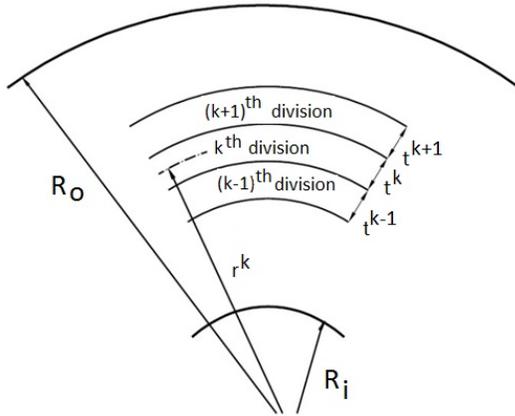
Fig. 2
Dividing radial domain into some finite sub-domains.

5 MAGNETO-THERMO-ELASTIC SOLUTION

The disk is placed in uniform magnetic field $\vec{H}(0,0,H_z)$ and rotating around its central axis with a constant angular velocity ω. The rotation creates a centrifugal acceleration and consequently centrifugal force that is used as body force through radius in equilibrium equation.

Since the disk is thin, the plane stress condition is considered. Moreover, cylindrical coordinate system is used and axial symmetry is assumed. For the axisymmetric plane stress problem, the constitutive relations are [4];

$$\varepsilon_{rr} = \frac{\mathrm{d}u}{\mathrm{d}r}, \qquad \varepsilon_{\theta\theta} = \frac{u}{r} \tag{17}$$

$$\sigma_r = \frac{E}{1-\nu^2}(\varepsilon_r + \nu\varepsilon_\theta - (1+\nu)\alpha_r\Delta T(r)) \tag{18a}$$

$$\sigma_\theta = \frac{E}{1-\nu^2}(\varepsilon_\theta + \nu\varepsilon_r - (1+\nu)\alpha_r\Delta T(r)) \tag{18b}$$

$$\sigma_{Von\_Mises} = \sqrt{\sigma_r^2 + \sigma_\theta^2 - \sigma_r\sigma_\theta} \tag{18c}$$

where α_r and σ_{Von_Mises} are thermal expansion coefficient and von-Mises stress, respectively. Assuming that magnetic permeability $\mu(r)$ is a power-law function of volume fraction according to Eq. (2). The governing Electro-Dynamic Maxwell Eqs. (15), (16) ,(17) for a perfectly conducting elastic body can be written as:

$$\vec{J} = \nabla \times \vec{h}, \qquad \nabla \times \vec{e} = -\mu(r)\frac{\partial \vec{h}}{\partial t}, \qquad\qquad div\,\vec{h} = 0,$$

$$\vec{e} = -\mu(r)\left(\frac{\partial \vec{U}}{\partial t} \times \vec{H}\right), \qquad \vec{h} = \nabla \times (\vec{U} \times \vec{H}) \tag{19}$$

Applying an initial magnetic field vector $\vec{H}(0,0,H_z)$ in the cylindrical coordinates to Eq. (19), yields:

$$\vec{U} = (u,0,0), \qquad \vec{e} = -\mu(r)\left(0, H_z \frac{\partial u}{\partial t}, 0\right),$$

$$\vec{h} = (0,0,h_z), \qquad \vec{J} = \left(0, -\frac{\partial h_z}{\partial t}, 0\right), \qquad h_z = -H_z\left(\frac{\partial u}{\partial r} + \frac{u}{r}\right) \tag{20}$$

The equilibrium equation of the FG hollow rotating disk under centrifugal body force is expressed as:

$$\frac{\partial \sigma_r}{\partial r} + \frac{\sigma_r - \sigma_\theta}{r} + f_z + \rho(r)r\omega^2 = 0 \tag{21}$$

where f_z is the Lorentz's force [9, 15, 18] as following:

$$f_z = \mu(r)(\vec{J} \times \vec{H}) = \mu(r)H_z^2 \frac{\partial}{\partial r}\left(\frac{\partial u}{\partial r} + \frac{u}{r}\right) \tag{22}$$

To obtain the equilibrium equation in terms of the displacement for the FG rotating disk, the functional relationships of the material properties have to be known. The variation of property along radius, as explained in sec. (2) is a power-law distribution of volume fraction:

$$E_r = E(r) = (E_o - E_i)\left(\frac{r - r_i}{r_o - r_i}\right)^n + E_i,$$

$$\alpha_r = \alpha(r) = (\alpha_o - \alpha_i)\left(\frac{r - r_i}{r_o - r_i}\right)^n + \alpha_i,$$

$$\rho_r = \rho(r) = (\rho_o - \rho_i)\left(\frac{r - r_i}{r_o - r_i}\right)^n + \rho_i, \tag{23}$$

$$\mu_r = \mu(r) = (\mu_o - \mu_i)\left(\frac{r - r_i}{r_o - r_i}\right)^n + \mu_i$$

Substituting property distribution Eq. (23) and stress relation Eqs. (18) into Eq. (21) yields an ODE in terms of radial displacement which is Navier's equation:

$$C_1 \frac{d^2 u}{dr^2} + C_2 \frac{du}{dr} + C_3 u + C_4 = 0 \tag{24}$$

where

$$C_1 = r(E(r) + \mu(r)H_z^2(1 - v^2))$$

$$C_2 = \mu(r)H_z^2(1 - v^2) + \frac{d}{dr}(rE(r))$$

$$C_3 = -\frac{1}{r}(E(r) + \mu(r)H_z^2(1 - v^2)) + v\frac{d}{dr}(E(r)) \tag{25}$$

$$C_4 = \rho(r)r^2\omega^2(1 - v^2) - r\frac{d}{dr}(E(r)(1 + v)\alpha_r(r)\Delta T(r))$$

It is shown that non-homogenous term C_4 of Eq. (24) is resulting of thermal field. According to the non-dimensional form Eq. (2), these relations can be written as:

$$\left(\overline{C_1}\frac{d^2}{dR^2}+\overline{C_2}\frac{d}{dR}+\overline{C_3}\right)U+\overline{C_4}=0 \tag{26}$$

where

$$\overline{C_1}=R(E_o\overline{E_R}+\mu_o\overline{\mu_R}H_z^2(1-v^2))$$

$$\overline{C_2}=\mu_o\overline{\mu_R}H_z^2(1-v^2)+E_o\frac{d(R\overline{E_R})}{dR}$$

$$\overline{C_3}=-\frac{1}{R}(E_o\overline{E_R}+\mu_o\overline{\mu_R}H_z^2(1-v^2))+vE_o\frac{d\overline{E_R}}{dR} \tag{27}$$

$$\overline{C_4}=\frac{\rho_o r_o^3\omega^2}{u_o}(1-v^2)\overline{\rho_R}R^2-\frac{r_o(T_i-T_\infty)}{u_o}R\frac{d(E_o\overline{E_R}(1+v)\alpha_o\overline{\alpha_R}\Delta T_R)}{dR}$$

and

$$U=\frac{u}{u_o}$$

$$u_o=\rho_o r_o^3\omega^2+E_o r_o(1+v)\alpha_o(T_i-T_\infty) \tag{28}$$

Eq. (26) is non-homogenous 2nd order ODE with variable coefficients. Similar to solution of heat conduction equation, the semi-analytical method must be employed.

The Navier's equation yields

$$\left(C_1^{(k)}\frac{d^2}{dR^2}+C_2^{(k)}\frac{d}{dR}+C_3^{(k)}\right)U^{(k)}+C_4^{(k)}=0 \tag{29}$$

The coefficients of Eq. (29) are evaluated in each division in terms of constants and the radius of kth division

$$C_1^{(k)}=R^{(k)}(E_o\overline{E_{R^{(k)}}}+\mu_o\overline{\mu_{R^{(k)}}}H_z^2(1-v^2))$$

$$C_2^{(k)}=\mu_o\overline{\mu_{R^{(k)}}}H_z^2(1-v^2)+E_o\left.\frac{d}{dR}\right|(R\overline{E_R})_{R=R^{(k)}}$$

$$C_3^{(k)}=-\frac{1}{R^{(k)}}(E_o\overline{E_{R^{(k)}}}+\mu_o\overline{\mu_{R^{(k)}}}H_z^2(1-v^2))+vE_o\left.\frac{d\overline{E_R}}{dR}\right|_{R=R^{(k)}} \tag{30}$$

$$C_4^{(k)}=\frac{\rho_o r_o^3\omega^2}{u_o}(1-v^2)\overline{\rho_{R^{(k)}}}(R^{(k)})^2-\frac{r_o(T_i-T_\infty)}{u_o}R^{(k)}\left.\frac{d}{dR}(E_o\overline{E_R}\alpha_o\overline{\alpha_R}(1+v)\overline{\Delta T_R})\right|_{R^{(k)}}$$

The closed-form solution for Eq. (29) can be written in the form of

$$U^{(k)}=X_1^{(k)}\exp(\eta_1^{(k)}R)+X_2^{(k)}\exp(\eta_2^{(k)}R)-\frac{C_4^{(k)}}{C_3^{(k)}} \tag{31}$$

where

$$\eta_1^{(k)},\eta_2^{(k)}=\frac{C_2^{(k)}\pm\sqrt{(C_2^{(k)})^2-4C_3^{(k)}C_1^{(k)}}}{2C_1^{(k)}} \tag{32}$$

Noting that this solution for Eq. (29) is valid in

$$R^{(k)} - \frac{t^{(k)}}{2} \le R \le R^{(k)} + \frac{t^{(k)}}{2} \tag{33}$$

and $X_1^{(k)}$ and $X_2^{(k)}$ are unknown constants for kth division.

As same as procedure which is explained in section 4, unknowns $X_1^{(k)}$ and $X_2^{(k)}$ are achieved by imposing the continuity conditions for distribution of radial displacement U and radial stress $\overline{\sigma_R}$. These conditions for each sub-domain at the interface are defined as:

$$
\begin{aligned}
U^{(k)}\Big|_{R=R^{(k)}+\frac{t^{(k)}}{2}} &= U^{(k)}\Big|_{R=R^{(k+1)}-\frac{t^{(k+1)}}{2}} \\
\overline{\sigma_R^{(k)}}\Big|_{R=R^{(k)}+\frac{t^{(k)}}{2}} &= \overline{\sigma_R^{(k)}}\Big|_{R=R^{(k+1)}-\frac{t^{(k+1)}}{2}}
\end{aligned}
\tag{34}
$$

Applying continuity conditions Eq. (34) and boundary conditions Eq. (5) and (6) yield a set of linear algebraic equations in terms of $X_1^{(k)}$ and $X_2^{(k)}$. The result of this set, determine the distribution of radial displacement U in each sub-domain according to Eq. (31). Consequently, the other parameters such as stresses and perturbation of magnetic field are calculated. In this semi analytical method, increasing number of divisions can improve accuracy of calculations.

6 NUMERICAL RESULTS AND DISCUTION

To illustrate the results of magneto-thermo-elastic solution in this study, a rotating FG disk with $R_0 = 5R_i$ is considered with non-dimensional form for material properties as explained in Sec. 2. Following Ghorbanpour et al. [9] the magnetic intensity is taken as $H_z = 2.23 \times 10^9$ A/m.

The analyses for two cases of hollow disk with free-free boundary condition and hollow disk with fixed-free boundary conditions have been carried out. The results for temperature, radial displacement, magneto-thermo-elastic stresses and the perturbation of the magnetic field vector for the FG rotating disk are presented. The following material properties are used in computing the numerical results [4, 7, 15]:

$$
\begin{aligned}
&E_i = 70\,\text{Gpa}, \qquad E_o = 151\,\text{Gpa} \\
&\rho_i = 2700\,\frac{\text{kg}}{\text{m}^3}, \qquad \rho_o = 5700\,\frac{\text{kg}}{\text{m}^3} \\
&\alpha_i = 23 \times 10^{-6}\,\frac{1}{{}^{\text{o}}\text{C}}, \qquad \alpha_o = 10 \times 10^{-6}\,\frac{1}{{}^{\text{o}}\text{C}} \\
&\mu_i = 1.256665081 \times 10^{-6}\,\frac{\text{H}}{\text{m}}, \qquad \mu_o = 2.63225901 \times 10^{-6}\,\frac{\text{H}}{\text{m}} \\
&K_i = 209\,\frac{\text{W}}{\text{m}\,{}^{\text{o}}\text{C}}, \qquad K_o = 20\,\frac{\text{W}}{\text{m}\,{}^{\text{o}}\text{C}} \\
&h = 10 \\
&v = 0.3 \\
&T_i = 200\,{}^{\text{o}}\text{C}, \qquad T_\infty = 30\,{}^{\text{o}}\text{C} \\
&\omega = 1200\,\text{rpm}
\end{aligned}
\tag{35}
$$

The value of grading index *n* in this solution is taken 0, 0.2, 0.5, 1.5 and infinity. Obviously, the zero value for *n* indicates full ceramic and infinity indicates full metal.

6.1 Magneto-thermo-elastic results
6.1.1 Free-free boundary condition

Fig. 3 illustrates the distribution of non-dimensional temperature versus dimensionless radius for various values of grading index *n*. It shows that thermal boundary condition at inner surface is satisfied for each grading index. Fig. 4 shows the variation of non-dimensional radial displacement versus radius for different value of grading index *n* . It can be seen from Fig. 4 that the displacement increases when the grading index decreases, so the maximum and minimum displacement are for full ceramic and full metal respectively. For all values of grading index n, the minimum displacement is located near the inner surface of the disk and its maximum is located near the outer surface of the disk. Fig.5 and 6 represent the variation of non-dimensional radial and circumferential stresses versus dimensionless radius respectively. The mechanical boundary conditions (free-free boundary conditions) are well satisfied in Fig. 5. As Figs. 5 and 6 show the maximum radial and circumferential stresses belong to full ceramic and their minimum values belong to full metal disk, and for FG disks these values are located between these two extremes.
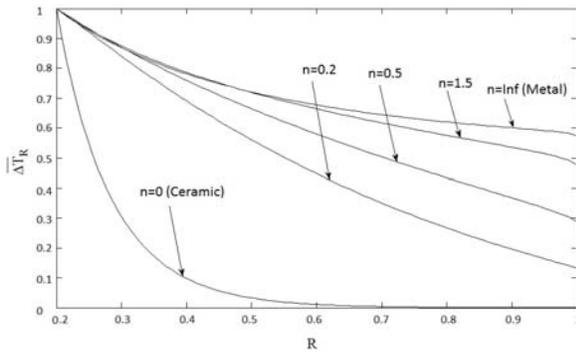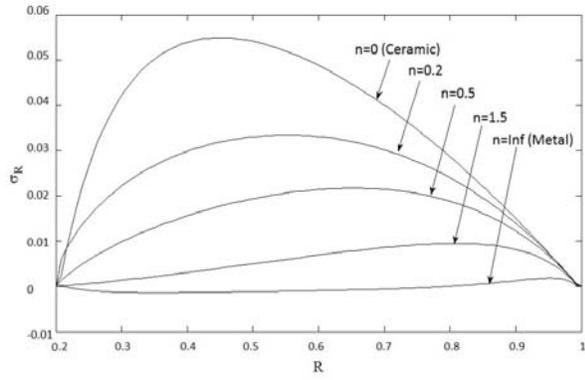

Fig. 3
Distribution of non-dimensional temperature difference along the radius of FG disk.
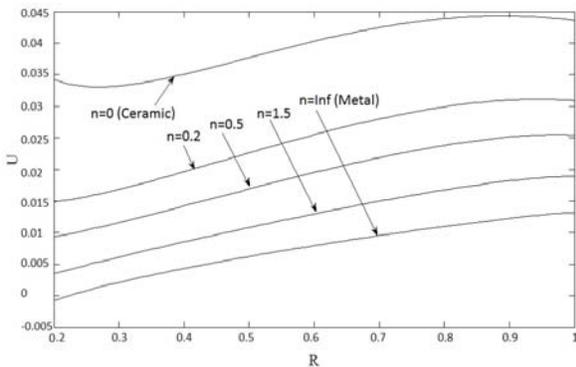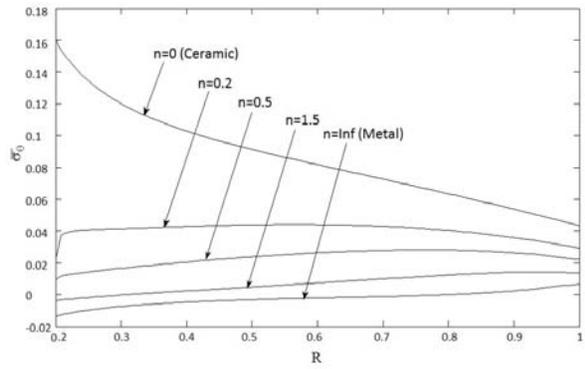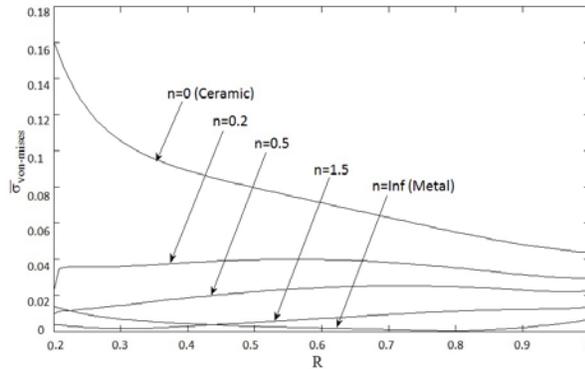

Fig. 4
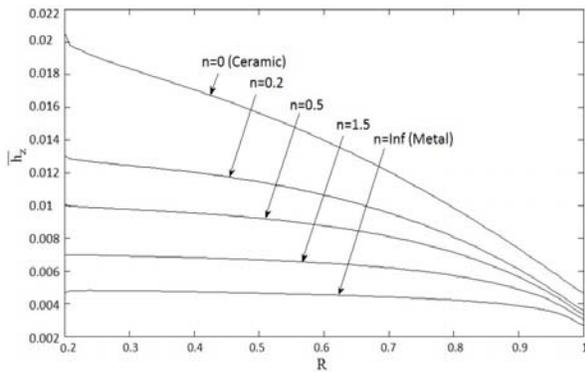Distribution of non-dimensional radial displacement for free-free boundary condition.

Fig. 5
Distribution of non-dimensional radial stress for free-free boundary condition.
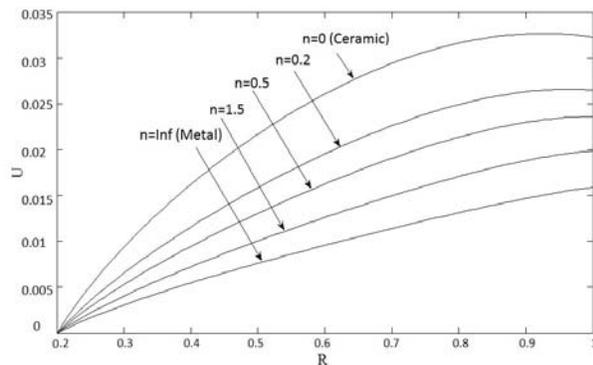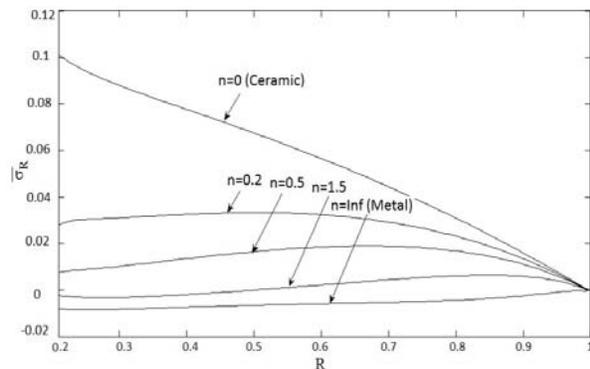

Fig. 6
Distribution of non-dimensional circumferential stresses for free-free boundary condition.

Fig. 7
Distribution of non-dimensional von-Mises stress for free-free boundary condition.

Fig. 8
Distribution of perturbation of magnetic field vector for free-free boundary condition.

Fig. 9
Distribution of non-dimensional radial displacement for fixed-free boundary condition.

Fig. 7 represents the variation of non-dimensional von-Mises stress versus radius for different value of grading index *n*. Distribution of non-dimensional perturbation of magnetic field vector versus dimensionless radius is shown in Fig. 8. It is seen form Fig. 8 that the magnitude of perturbation of magnetic field vector decreases with increasing the grading index n. The perturbation of magnetic field vector smoothly decreases from its maximum value at the inner surface to its minimum value at the outer surface of the disk for all grading index.
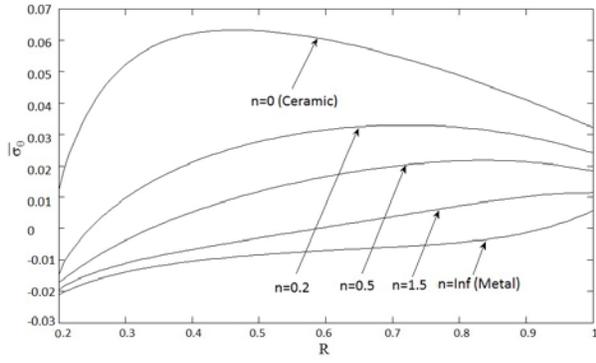
6.1.2 Fixed-free boundary condition

The results presented here in this section are according to the fixed-free boundary conditions Eq. (6). Obviously, the non-dimensional temperature distribution is the same as free-free boundary condition case Fig. 3.

The non-dimensional radial displacement versus dimensionless radius is illustrated in Fig. 9. It shows that increasing grading index *n* from full ceramic to full metal decreases the radial displacement. Clearly, the boundary condition of displacement at the fixed inner surface is satisfied in Fig. 9. Maximum displacements occur at the outer surfaces of the disks for all grading indexes from ceramic to metal. Figs. 10 and 11 show the distribution of non-dimensional radial and circumferential stresses, respectively. In both cases, the maximum values belong to ceramic and the minimum values belong to metal. For FG disks, based on their grading index, their stress distribution are located between metal and ceramic extremes. As Fig. 10 shows the radial stresses are maximum at the near inner surface of the disks for all grading indexes because of the fixed boundary condition at the inner surface of the disks, however their minimum zero values at the outer surfaces satisfy the free boundary condition at the outer surfaces.

Fig. 12 represents the variation of non-dimensional von-Mises stress versus radius for different value of grading index n. The distribution of non-dimensional perturbation of magnetic field vector is shown in Fig. 13. It shows that the variation of perturbation of magnetic field vector is almost the same as Fig. 8, approximately.
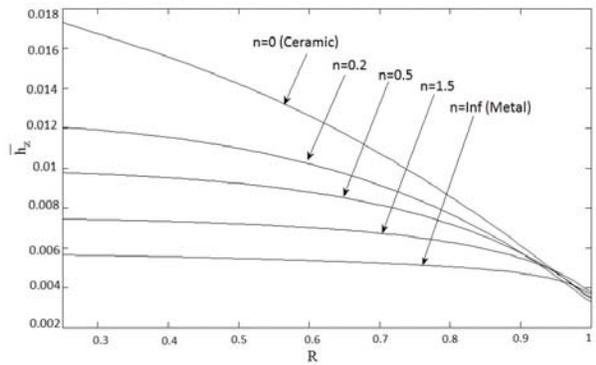

Fig. 10
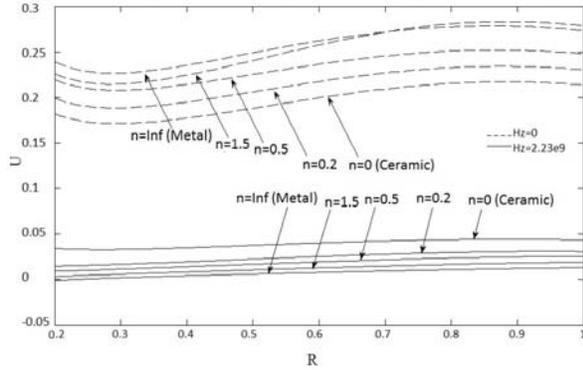Distribution of non-dimensional radial stress for fixed-free boundary condition.

Fig. 11
Distribution of non-dimensional circumferential stress for fixed-free boundary condition.
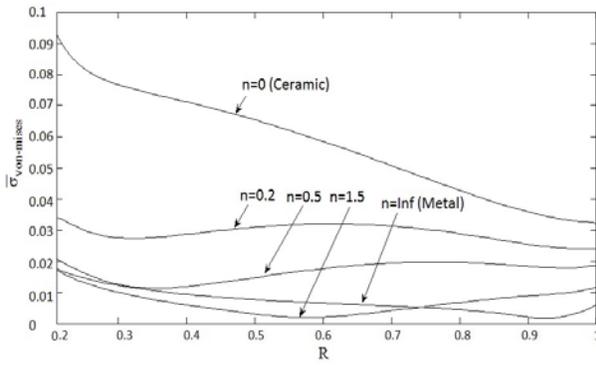
Fig. 12
Distribution of non-dimensional von-Mises stress for fixed-free boundary condition.

Fig. 13
Distribution of perturbation of magnetic field vector for fixed-free boundary condition.

Fig. 14
Comparing non-dimensional radial displacement with and without considering magnetic field for free-free boundary condition.
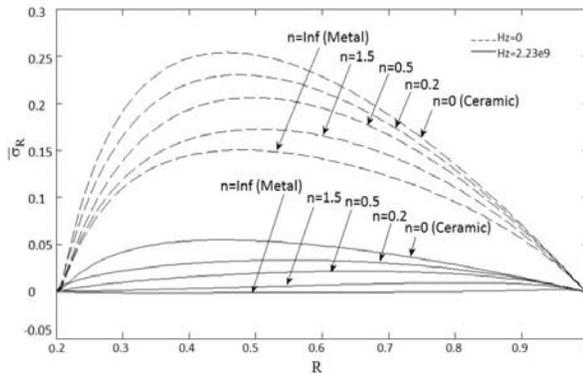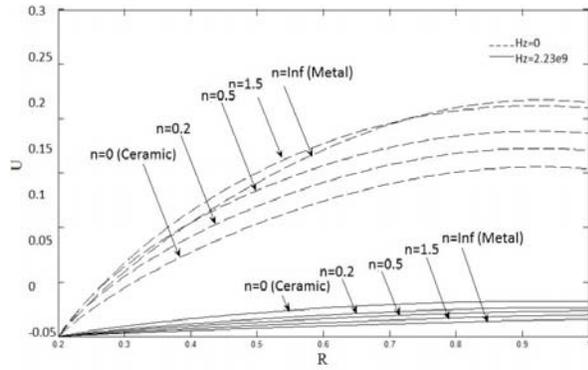

Fig. 15
Comparing non-dimensional radial stress with and without considering magnetic field for free-free boundary condition.

6.2 Comparison of magneto-thermo-elastic solution with thermo-elastic solution

In order to investigate the effect of uniform magnetic field on mechanical behavior of the disk, the semi-analytical solution has also been carried out in the absence of magnetic field in order to compare these two cases.
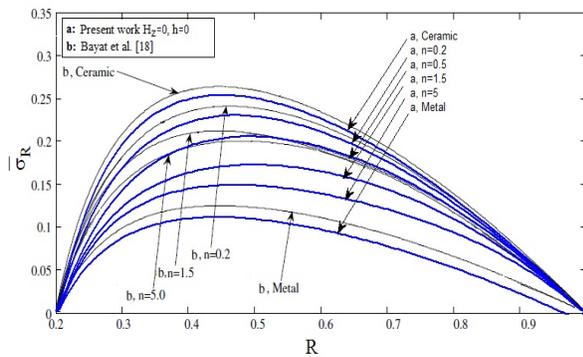
6.2.1 Free-free boundary condition

Based on Sec. 4, the thermal analysis is independent on magnetic field and the magnetic field has no effect on thermal analysis. Thus, the distribution of non-dimensional temperature difference along radius is the same as shown before in Fig. 3. Fig. 14 illustrates non-dimensional radial displacement variation throughout dimensionless radius, with and without considering the magnetic field. It shows that applying the uniform magnetic field reduces radial displacement. Distributions of non-dimensional radial stresses are shown in Fig. 15. It can be seen in both graphs that magnetic field significantly reduces the value of stresses. As Fig. 15 shows, the order of grading index from metal to ceramic has been kept the same whether being magnetic field or not.

Fig. 16
Comparing non-dimensional radial displacement with and without considering magnetic field for fixed-free boundary condition.
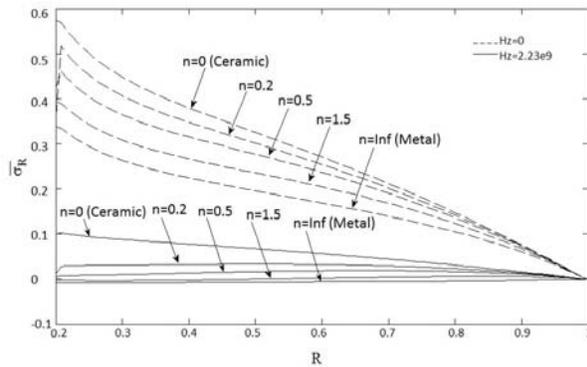
Fig. 17
Comparing non-dimensional radial stress with and without considering magnetic field for fixed-free boundary condition.

Fig. 18
Comparison non-dimensional radial stress between present work with those presented by Bayat et al. [18].

6.2.2 Fixed-free boundary condition

The variation of non-dimensional radial displacement and radial stresses along radius are illustrated in Figs. 16 and 17 respectively. The boundary condition of zero displacement at the inner fixed condition is satisfied in Fig. 16 and the boundary condition of zero radial stress at the outer free surface of the disk is also satisfied in Fig. 17. It is obvious from Fig. 17 that for this case, the discussion of previous section is valid.

6.3 Result validation

In order to validate the present study, a simplified case of the analysis is considered by neglecting magnetic filed (H_z=0) and convection heat transfer (h=0). The results presented by Bayat et al. [18] are compared with the results of this investigation, in Fig. 18 which shows a very good agreement for non-dimensional radial stress.

7   CONCLUSIONS

A semi-analytical solution for magneto-thermo-elasticity equilibrium equations and steady state conduction and convection heat transfer of a thin axisymmetric functionally graded rotating disk is presented. The effects of constitutive gradation properties along radius, on stresses, displacement, temperature, and perturbation of magnetic field vector of the FG rotating disk have been investigated. The results of stresses and displacements with and without considering the magnetic field for two different boundary conditions are compared. The following conclusions can be drawn from the present study:

1. Distribution of temperature, stresses, displacement and perturbation of magnetic field are located between these two extremes of metal and ceramic for different values of grading index.
2. From the semi-analytical results for FG disks given in this study, it can be suggested that the gradation of the metal–ceramic components are significant parameters in the magneto-thermo-mechanical responses of rotating FG disks.
3. Except for displacement, applying magnetic field does not change the location order of grading index.
4. The results of stresses and displacements for FG rotating disk with and without considering the magnetic field for two different boundary conditions are compared. It has been found that a uniform magnetic field significantly decreases the von-Mises equivalent stresses, the tensile circumferential and radial stresses as well as the radial displacement. Therefore, the fatigue life of such components can be significantly improved by imposing a magnetic field.

ACKNOWLEDGMENTS

REFERENCES

[1]   Suresh S., Mortensen A.., 1998, Fundamentals of functionally graded materials, London, UK: IOM Communications Limited.
[2]   Lutz M.P., Zimmerman R.W., 1966, Thermal stresses and effective thermal expansion coefficient of a functionally graded sphere, *Journal Thermal Stresses* **19**: 39-54.
[3]   Zimmerman R.W., Lutz M.P., 1999, Thermal stresses and effective thermal expansion in a uniformly heated functionally graded cylinder, *Journal Thermal Stresses* **22**: 177-188.
[4]   Kordkheili S.A.H., Naghdabadi R., 2007, Thermoelastic analysis of a functionally graded rotating disk, *Composite Structures* **79**:508-516.
[5]   Obata Y., Noda N., 1994, Steady thermal stresses in a hollow circular cylinder and a hollow sphere of a functionally gradient material, *Journal Thermal Stresses* **17**: 471-488.
[6]   Dai H.L., Fu Y.M., 2007, Magneto thermoelastic interaction in hollow structures of functionally graded material subjected to mechanical loads, *International Journal of Pressure Vessels and Piping* **84**: 132-138.
[7]   Dai H.L., Fu Y.M., Dong Z.M., 2006, Exact solution for functionally graded pressure vessels in a uniform magnetic field, *International Journal of Solids and Structures* **43**: 5570-5580.
[8]   Ghorbanpour Arani A., Salari M., Khademizadeh H., Arefmanesh A., 2010, Magneto thermoelastic transient response of a functionally graded thick hollow sphere subjected to magnetic and thermoelastic fields, *Journal of Achieve of Applied Mechanics* **79:** 481-497.
[9]   Ghorbanpour Arani A., Salari M., Khademizadeh H., Arefmanesh, A., 2010, Magneto thermoelastic stress and perturbation of magnetic field vector in a functionally graded hollow sphere, *Journal of Achieve of Applied Mechanics* **80**: 189-200.
[10]   Tang S., 1968, Elastic stresses in rotating anisotropic disks, *International Journal of Mechanical Sciences* **11**: 509-517.
[11]   Ruhi M., Angoshtari A., Naghdabadi R., 2005, Thermoelastic analysis of thick-walled finite-length cylinders of functionally graded materials, *Journal Thermal Stresses* **28**: 391-408.

[12]   Farshi B., Jahed H., Mehrabian A., 2004, Optimum design of inhomogeneous nonuniform rotating disks, *International Journal of Computers and Structures* **82**: 773–779.

[13]   Loghman A., Ghorbanpour Arani A., Amir S., Vajedi A., 2010, Magneto thermoelastic creep analysis of functionally graded cylinder, *International Journal of Pressure Vessels and Piping* **87**: 389-395.

[14]   Bayat M., Sahari B.B., Saleem M., Aidy A., Wong S.V., 2009, Thermoelastic solution of a functionally graded variable thickness rotating disk with bending based on the first-order shear deformation theory, *Thin-Walled Structures* **47**: 568-582.

[15]   Ghorbanpour Arani A., Loghman A., Shajari A.R., Amir S., 2010, Semi-analytical solution of magneto-thermo-elastic stresses for functionally graded variable thickness rotating disks, *Journal of Mechanical Science and Technology* **24**: 2107-2118.

[16]   Kraus J.D., 1984, *Electromagnetic*, McGraw-Hill, New York.

[17]   Paul C.R., Nasar S.A., 1987, *Introduction to Electromagnetic Fields*, Mc. Grawhill, Second Edition.

[18]   Bayat M., Saleem M., Sahari B.B., Hamouda A.M.S., Mahdi E., 2009, Mechanical and thermal stresses in a functionally graded rotating disk with variable thickness due to radially symmetry loads, *International Journal of Pressure Vessels and Piping* **86**: 357-372.